International Journal of Materials Research 105 (2014) 1166-1172

Segregation of phosphorus to ferrite grain boundaries during transformation in Fe–P alloy

Jeong In Kim[a], Jun Hak Pak[b], Kyong-Su Park[b], Jae Hoon Jang[b], Dong-Woo Suh[a], H. K. D. H. Bhadeshia[a,c]

[a] *Graduate Institute of Ferrous Technology, POSTECH, Republic of Korea*

[b] *Technical Research Laboratories, POSCO, Republic of Korea*

[c] *Materials Science and Metallurgy, University of Cambridge, U.K*

Abstract

A binary alloy of iron containing 0.17 wt% of phosphorus has been heat-treated under a variety of conditions in order to see whether the segregation of phosphorus to grain boundaries can be controlled. The alloy transforms fully into ferrite. It is found that the majority of solute found at the ferrite grain boundaries has its origins in the temperature range where phase transformation occurs, in other words, phosphorus that is accumulated and dragged with the growing α/γ transformation front. As a consequence, it cannot be suppressed using cooling rates as large as $400\,\mathrm{K\,s^{-1}}$.

Keywords: Phosphorus, segregation, grain boundary, ferrite, austenite

1. Introduction

The segregation of impurities to grain boundaries, and the thermodynamics of the process have been studied extensively [1–3], [4, reviewed in]. The problem is important, in part because of the deleterious consequences of such segregation on mechanical properties [5–8]. The enrichment of the impurities at boundaries reduces their cohesive strength, leading in some circumstances to intergranular fracture under load [9–11]. Phosphorus is particularly po-

Email address: dongwoo1@postech.ac.kr (Dong-Woo Suh)

tent in this respect [12], causing grain boundary embrittlement when a strong steel is tempered or cooled slowly through a temperature range 600-650°C [9, 13], or the so-called tempered martensite embrittlement at 300-350°C due to the segregation at cementite-ferrite interfaces [14–16].

From an experimental and theoretical point of view, phosphorous segregation has been characterised for static boundaries, such as those between austenite (γ) grains or ferrite (α) grains [17–20] or interfaces between cementite and ferrite [21]. One aspect that to our knowledge has never been studied, is what happens to the phosphorus that is at γ/γ boundaries when allotriomorphic ferrite forms. This phase transformation is reconstructive in nature and hence is not limited by the original γ/γ boundary, which can be destroyed completely as the ferrite grows into both of the adjacent austenite grains.

It is possible that the phase transformation renders the phosphorus benign by leaving it in positions away from boundaries. The issue is now of increasing importance given that there are concerted efforts to exploit the solution strengthening of ferrite using phosphorus as a solute [22–24]. The purpose of the present work was to investigate the segregation behaviour of phosphorous to ferrite grain boundaries on cooling from the austenitisation temperature in a binary Fe-P alloy. The segregation behaviour has been examined using a variety of cooling patterns designed to quantify phosphorous segregation effects in the context of reconstructive transformation.

2. Experimental technique

The composition of investigated alloy is Fe-0.17P-0.004C-0.018Mn-0.004Si (wt%). An ingot made using a vacuum-induction furnace, was reheated to 1473 K for 2 h followed by hot-rolling in the temperature range 1273-1373 K, into 10 mm in thick plate followed by air-cooling to room temperature. Rectangular specimens 4 $\times$4 $\times$ 16 mm and a cylindrical specimen 8 mm in diameter and 16 mm long, were machined from the hot-rolled plate for heat treatment using a dilatometer and thermomechanical simulator, respectively. Heat treatments (Fig 1) which involved cooling at rates up to 100 K s^{-1} were conducted using the dilatometer, and those requiring water quenching on the thermomechanical simulator. All the specimens were austenitised at T_γ =1373 K for 30 min. In cooling pattern A, the specimens were cooled to

room temperature at constant cooling rates of 1, 3, 20, 100 $\mathrm{K\,s^{-1}}$. Water quenching gave a cooling rate of $\approx 400\,\mathrm{K\,s^{-1}}$. In pattern B, the specimens were cooled at a specified rate to the temperature where the ferrite transformation completes, then further cooled to room temperature at $100\,\mathrm{K\,s^{-1}}$. The transformation-finish temperatures were determined from the dilatometric curves shown in Fig. 1d. In pattern C, the specimens were cooled at $1\,\mathrm{K\,s^{-1}}$ to the transformation-finish temperature, followed by subsequent cooling to room temperature at 1, 3, 20, 100 $\mathrm{K\,s^{-1}}$.

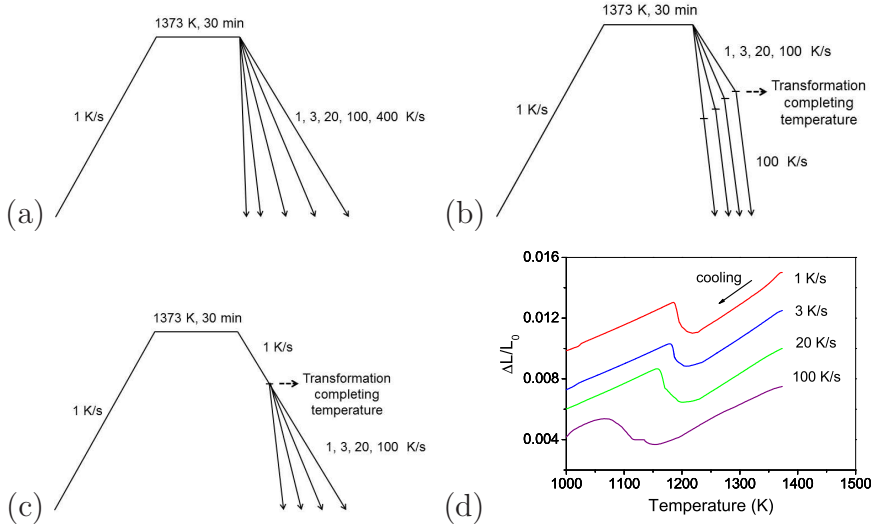

Figure 1: Heat treatment patterns (a) A, (b) B (c) C, (d) dilatation curves.

The concentration of phosphorous at ferrite grain boundaries was evaluated by means of Auger Electron Spectroscopy (AES). The spectroscope (PHI 700) was operated with a primary energy of 5 keV, at a vacuum of 6×10^{-10} torr, with an emission current of 90 μA and an electron beam size of about 300 nm.

The heat treated sample was machined into $3 \times 1.5 \times 16$ mm rectangular specimen with a notch. It was kept in liquid nitrogen in the AES chamber for 30 min and immediately fractured to obtain fresh, intergranular-fracture surfaces. The AES peaks used for analysis were $\mathrm{Fe_{703}}$, $\mathrm{P_{120}}$ and $\mathrm{C_{271}}$. The concentration on the fractured surface was estimated as follows [25]:

$$C_i = \frac{H_i/S_i}{\sum_k H_k/S_k} \tag{1}$$

where H and S denote the Auger peak height and sensitivity factor; the latter is 0.205, 0.613 and 0.128 for Fe, P and C, respectively. This method is semi-quantitative because it neglects variations in the backscattering factor and escape depth within the material, so the absolute values of phosphorus concentration are likely to be underestimated. However, for the purposes of the present study it is not necessary to measure the true concentration but rather the value at the grain boundary relative to that in the matrix. The grain boundary concentration was estimated as twice the measured surface concentration. Since AES results show a considerable scatter, the analysis errors are given ± 95 % double side confidence interval on the mean value [25].

For the microstructural characterisation using optical microscopy, the specimen was prepared using a standard method with 2 % nital etchant. The grain size of ferrite was determined by as a mean lineal intercept since this parameter is related directly to the grain surface per unit volume.

3. Results and Discussion

3.1. Segregation during cooling from austenitising temperature

Fig. 2 shows an example of a fracture surface; the associated spectra confirm that while the segregation of phosphorus and carbon is present at the ferrite-ferrite intergranular surface, both solutes are as expected, absent at the cleavage facet. It is noted that there is a small oxygen peak at about 510 eV, but this was present in both the intregranular and transgranular spectra and hence probably originates from the gas within the equipment rather than from the specimen itself.

To examine the possibility that the segregation detected is at a prior austenite grain boundary, thermal grooving experiments were done by metallographically preparing a sample and then subjecting it to the austenitisation treatment in a vacuum, followed by quenching into water. The grain boundary grooves together with oxide etching revealed the γ/γ boundaries (Fig. 3a) and mean lineal intercepts gave size of 67±6 μm where the standard error quoted is for 95% confidence. The same sample was then lightly polished in order to preserve vestiges of the grooves, followed by light etching with nital to reveal the ferrite boundaries. Fig. 3b shows clearly that the ferrite grains grow across the austenite grain boundaries. Furthermore,

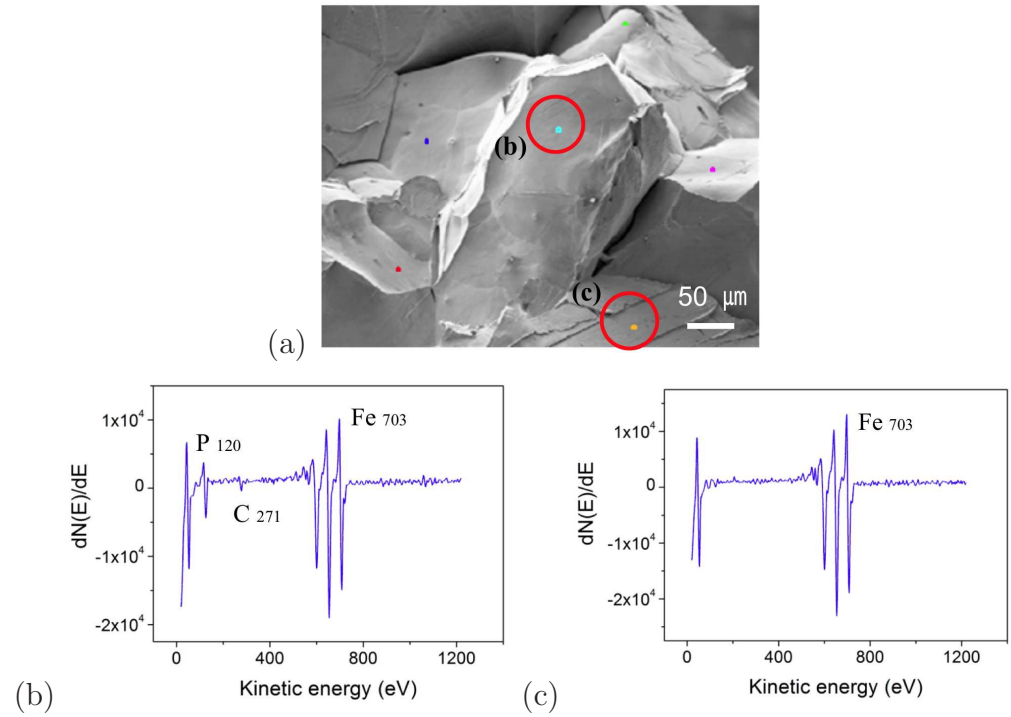

Figure 2: (a) Fracture surface of AES sample cooled at $1\,\mathrm{K\,s^{-1}}$ according to pattern A in Fig. 1. (b) Spectrum from intergranular surface. (c) Spectrum from cleavage facet.

the former γ/γ boundaries are not attacked by the etchant, which is not surprising since they do not exist other than the region of ferrite that has retained some of the thermal grooving introduced at elevated temperatures. Quantitative data on ferrite grain sizes are reported later in the paper, and in all cases are much larger than the austenite grain size, but comparable in size to the fracture facets.

Fig. 4a shows the atomic fraction of phosphorous at ferrite grain boundaries subjected to heat treatment A. The phosphorous segregation decreases gradually as the cooling rate increases. However, even with the highest cooling rate of $400\,\mathrm{K\,s^{-1}}$ where the ferritic structure shown in Fig. 4d is still obtained, the segregation of phosphorous is 0.118 atomic fraction, which is 80% of the maximum segregation level of 0.146 atomic fraction at a cooling rate of $1\,\mathrm{K\,s^{-1}}$. This indicates that the segregation of phosphorous in ferrite grain boundaries is not significantly avoided by accelerated cooling from the austenitising temperature over the range of cooling rates studied.

Fig. 4b shows the data for heat treatment B, where samples were cooled rapidly to room temperature at $100\,\mathrm{K\,s^{-1}}$ after the decomposition of austenite (γ) to ferrite (α) was completed. The diffusion distance of phosphorus in ferrite during cooling at this rate and after completing the transformation can be approximated as [26],

$$d^2 = 6\int_0^{t_a} D\ dt \tag{2}$$

where t is the time to be zero at the point where phase transformation to ferrite finishes, and t_a when the sample reaches ambient temperature. This time period covers the temperature range T_f to 298 K (25°C). The diffusivity for phosphorus in ferrite is given by $D_{\mathrm{P}}^{\alpha} = 0.0071\times10^{-4}\exp\{-167500/RT\}\mathrm{m^2\,s^{-1}}$ [27]; R is the gas constant and T the absolute temperature. Using this equation, the diffusion distance over the cooling period is found to be just 0.37 μm, a value that is an order of magnitude small than the grain size of the ferrite. It is therefore reasonable to assume that the segregation of phosphorus during the cooling from T_f at $100\,\mathrm{K\,s^{-1}}$ is not possible. It follows that the segregation must have occurred during the $\gamma \rightarrow \alpha$ transformation itself at temperatures above T_f, consistent with the fact that the extent of segregation is essentially constant at 0.13 atomic fraction for all the cooling rates below T_f.

It is suggested here that the phosphorus segregation may occur as the α/γ

(a)

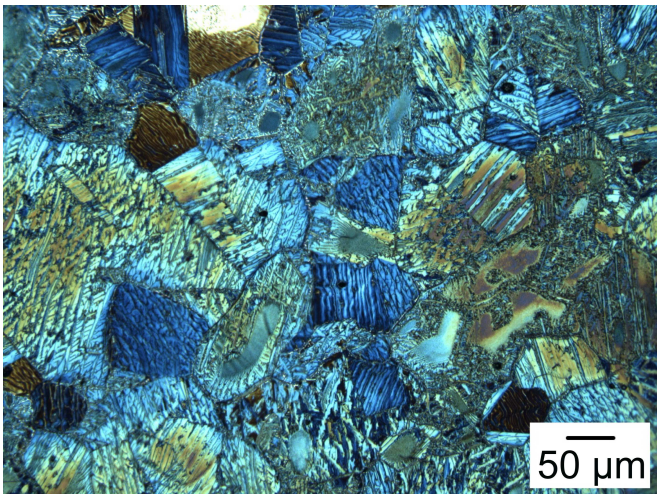

(b)

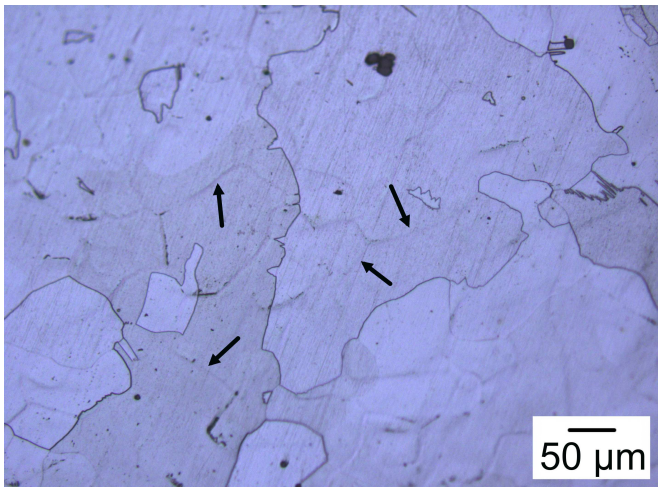

Figure 3: (a) Thermal grooves as well as oxide-etching reveal the austenite grain boundaries; (b) The same sample, lightly polished and lightly etched with nital, to reveal the ferrite grain boundaries and vestiges of the austenite grain boundary grooves.

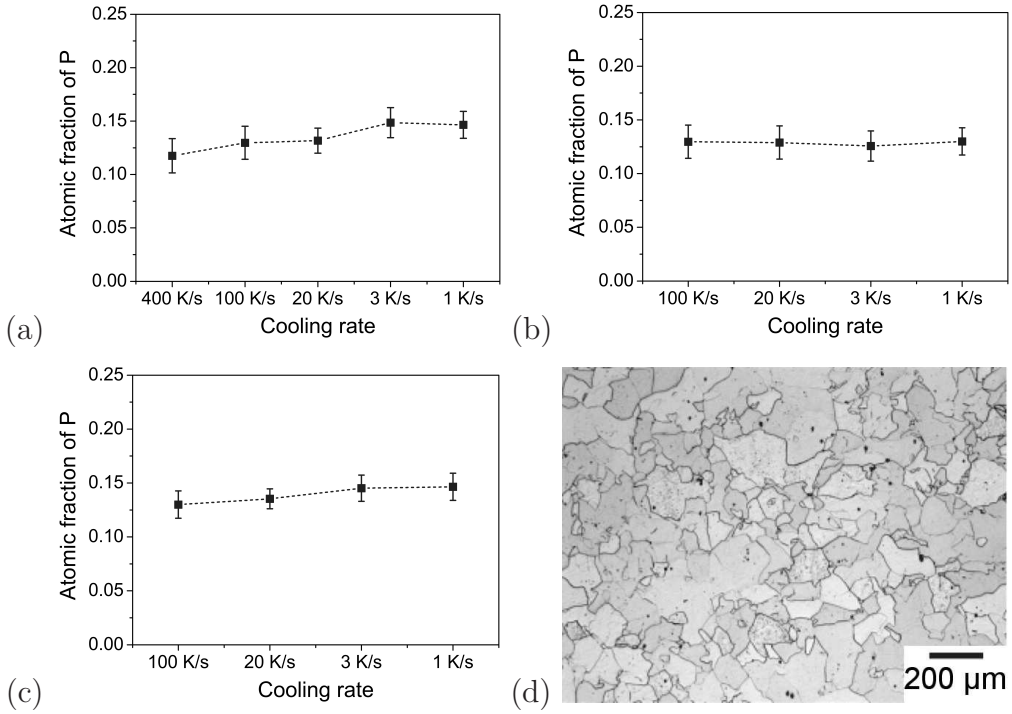

Figure 4: Atomic fraction of phosphorous in grain boundary. (a) pattern A, (b) pattern B, (c) pattern C, (d) optical microstructure of specimen cooled at $400\,\mathrm{K\,s^{-1}}$.

interphase boundary advances during transformation. If it is assumed that for the heat-treatment pattern A, where the samples are continuously cooled from the austenitisation temperature, the measured phosphorus concentration (x_A) whereas in pattern B the concentration (x_B) is due to segregation above T_f, then the difference $x_A - x_B$ represents segregation below T_f. Comparison of the data from heat treatments A and B, Table 2, shows that the segregation during the cooling of ferrite is insignificant.

Table 1: Quantitative data relating to Fig. 4.

Sample	Cooling rate / $\mathrm{K\,s^{-1}}$	Atomic fraction P	95% confidence interval
Fig. 4a	400	0.11752	0.01602
Fig. 4a	100	0.12969	0.0154
Fig. 4a	20	0.13167	0.01167
Fig. 4a	3	0.14853	0.01411
Fig. 4a	1	0.14643	0.01258
Fig. 4b	400	0.11752	0.01602
Fig. 4b	100	0.12969	0.0154
Fig. 4b	20	0.13167	0.01167
Fig. 4b	3	0.14853	0.01411
Fig. 4b	1	0.14643	0.01258
Fig. 4c	100	0.12997	0.01265
Fig. 4c	20	0.13535	0.00923
Fig. 4c	3	0.14512	0.01215
Fig. 4c	1	0.14643	0.01258

Table 2: Segregation of phosphorous during and after phase transformation. Concentrations x are presented as atomic fractions.

	Cooling rate from $T_\gamma = 1373\,\mathrm{K}$			
	$100\,\mathrm{K\,s^{-1}}$	$20\,\mathrm{K\,s^{-1}}$	$3\,\mathrm{K\,s^{-1}}$	$1\,\mathrm{K\,s^{-1}}$
Pattern B, segregation during $\gamma \to \alpha$ change, x_B	0.130	0.129	0.126	0.130
Segregation during cooling below T_f, $x_A - x_B$	0	0.003	0.022	0.016

These results are confirmed by the phosphorous segregation during heat treatment C in Fig. 4c, where the cooling rates below T_f are varied in order to check whether the level of segregation changes while the sample is fully

Table 3: Segregation of phosphorous during phase transformation and cooling in ferrite regime estimated from AES analysis on heat treatment pattern C

	$100\,\mathrm{K\,s^{-1}}$	$20\,\mathrm{K\,s^{-1}}$	$3\,\mathrm{K\,s^{-1}}$	$1\,\mathrm{K\,s^{-1}}$
Segregation during $\gamma \rightarrow \alpha$ change during cooling at $1\,\mathrm{K\,s^{-1}}$	0.13	0.13	0.13	0.13
Segregation during cooling at different rates below T_f, $x_C - 0.13$	0	0.005	0.015	0.016

ferritic. The cooling rate above T_f was maintained at $1\,\mathrm{K\,s^{-1}}$ for all samples, so the amount of phosphorus segregated during transformation can be taken to be 0.13 atomic fraction (Fig. 4c). Table 3 shows the difference $0.13 - x_C$, the estimated contribution of phosphorous segregation during the cooling of ferrite to the overall grain boundary concentration; the results are consistent with those in Table 2, which suggests that the segregation of phosphorous during the $\gamma \rightarrow \alpha$ transformation dominates the overall grain boundary concentration of phosphorus in ferrite.

3.2. Grain size effect

In any grain boundary segregation problem, provided that saturation does not occur before the solute within the grains is exhausted, the concentration of phosphorus detected will depend on the grain size [28]. An analysis was therefore conducted to assess whether the results are affected by difference in the ferrite grain size as a function of the heat treatment. The grain size effect on the equilibrium segregation is expressed by following equation.

$$\frac{x_b}{x_b^o - x_b} = \frac{\overline{x} - (3t/2r)x_b}{1 - \overline{x}} \ \exp\left\{-\frac{\Delta G}{RT}\right\} \tag{3}$$

where, x_b and x_b^o are the solute concentrations at the grain boundary and at saturation, and $\overline{x}$ is the bulk concentration. The terms t, r and ΔG represent grain boundary thickness, average grain radius and the free energy of segregation, respectively. When $\overline{x}$ is comparable to the $(3t/2r)x_b$, the grain size has an influence on the segregation, but if $\overline{x} \gg (3t/2r)x_b$, then the effect of grain size on the segregation behaviour will be negligible. For the evaluation of the grain size effect in the present study on Fe–0.17P alloy, we assume a monolayer of phosphorous ($x_b^o = 1$) [9], t to be 1 nm [28] and $\Delta G = -34300 - 21.5 \times T$ (J mol^{-1} K^{-1}) [9]. As shown in Fig. 5a, there is essentially no difference in equilibrium segregation level of phosphorous when the grain size of ferrite changes from 10 – 1000 μm, in the Fe-0.17P wt% alloy.

This is attributed to the fact that there is an exceptionally large concentration of phosphorus in the alloy, which leads to $\overline{x} \gg (3t/2r)x_b$. Therefore, over the grain size (measured as a mean lineal intercept) range relevant in the present work, 100 – 200 μm in Fig. 5b, any grain size effect can be neglected.

Note that the original work quoted in Eq. 3 refers to grain size at a grain radius estimated assuming the grain is spherical. A truncated octahedron is a better representation of a space-filling grain shape, in which case the mean lineal intercept is given by $\overline{L} = 1.69a$ where a is the edge length [29], and the volume of the octahedron is given by $11.314a^3$. By comparing the volumes of a sphere and the truncated octahedron, we obtain $\overline{L} = 1.21r$. This is the reason for the factor of 1.21 in Fig. 5a.

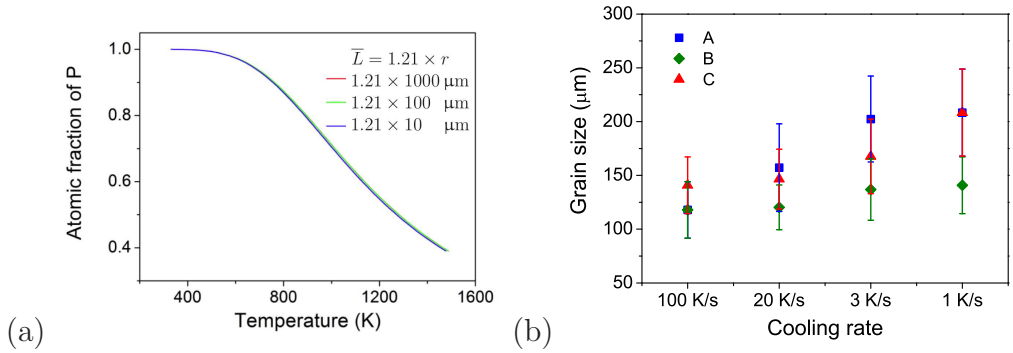

Figure 5: (a) Effect of grain size (mean lineal intercept) on the equilibrium segregation; there are three curves that are so similar that they cannot be distinguished, indicating an insensitivity of segregation to grain size. (b) Average grain size after heat treatment

3.3. Segregation during transformation

The Auger analysis implies that most of the phosphorous segregation into grain boundary of ferrite is likely to take place during the austenite to ferrite transformation. The boundary is effectively a solute trap whether or not it is stationary [30, 31], and it is noteworthy that allotriomorphic ferrite nucleates at the austenite grain boundaries so there is a ready source of segregated phosphorus available at its genesis.

However, for the segregation to persist during transformation, it is necessary for the solute to keep pace with the moving boundary. The α/γ boundary will move during transformation through a distance approximately half

the grain size. Using Eq. 2, the diffusion distance of phosphorus over the same temperature history as experienced by the ferrite [1], can be evaluated. It is noted that t is the time for the completion of transformation and D is diffusivity at migrating interface in this case. Since the diffusivity in the migrating α/γ interface is not available, we adopted the coefficient for diffusion parallel to an α/α grain boundary: $D_{\parallel}^{B} = 8.65 \times 10^{-4} \exp\{-153000/RT\} \mathrm{m}^2\,\mathrm{s}^{-1}$ [32]. The results are presented in Fig. 6 which compares the distance of interface migration during phase transformation and the diffusion distance of phosphorous on the basis of $D_{\parallel}^{B}$. It is clear that the diffusion distances are comparable to the migration distance of interface except for the fastest cooling rate of $100\,\mathrm{K\,s}^{-1}$, which implies that the concentration spike possibly keep pace with the migration of interphase boundary.

There have been suggestions that the diffusion coefficient for migration across an α/γ interface should lie between that for the lattice diffusivities of ferrite and austenite, although the precise location within the domain $D^{\alpha} > D_{\perp} > D^{\gamma}$ is not known [33]. A later publication [34] assumes a geometric average ($D_{\perp} = \sqrt{D^{\alpha} \times D^{\gamma}}$), attributing this to [33] but Hutchinson et al. do not in fact propose this relationship, nor is the value of $D_{\perp}$ that they settled on consistent with the geometric mean. It also seems that during recrystallisation, $D_{\perp}$ is related more closely to bulk diffusion rather than $D_{\parallel}$ [35]. The lattice diffusion coefficients are given by $D_{\mathrm{P}}^{\alpha} = 0.0071 \times 10^{-4} \exp\{-167500/RT\} \mathrm{m}^2\,\mathrm{s}^{-1}$ and $D_{\mathrm{P}}^{\gamma} = 0.01 \exp\{-184200/RT\} \mathrm{m}^2\,\mathrm{s}^{-1}$ [27]. Using these values of lattice diffusivities leads to the result that in no case does the diffusion distance exceed $3.2\,\mu\mathrm{m}$ even for the slowest cooling rate, which clearly is not consistent with the present observation that the phosphorus is present at the α/α boundaries.

There is no fundamental justification for assuming that $D^{\alpha} > D_{\perp} > D^{\gamma}$; the notion has its origins in the analysis of some complex data that assume the one-dimensional thickening of particles which in reality are not layers, and then fitting a mobility value to the data [33]. On the other hand, it is known that the thermodynamic properties of the migrating interface may be taken to be identical to those of a liquid phase [36, 37], and that the diffusivity at the migrating boundary is calculated to be 3 – 4 orders greater

[1] The temperature ranges for the calculations are as follows: (a) $1\,\mathrm{K\,s}^{-1} : 1228 - 1183\,\mathrm{K}$, (b) $3\,\mathrm{K\,s}^{-1} : 1228 - 1178\,\mathrm{K}$, (c) $20\,\mathrm{K\,s}^{-1} : 1228 - 1148\,\mathrm{K}$, (d) $100\,\mathrm{K\,s}^{-1} : 1198 - 1038\,\mathrm{K}$

than that of stationary boundary [38]. Indeed, there is a lot of accumulated evidence in the context of diffusion-induced boundary migration that the moving-boundary diffusivity is orders of magnitude greater than for stationary boundaries [39–41] and the reasoning has a physical mechanism on the basis of the nature of atomic jumps in the two scenarios [40]. It is therefore felt that in the absence of data on the anisotropy of boundary diffusivities, it is reasonable to use $D_{\parallel}^{B}$ in the analysis presented in Fig. 6.

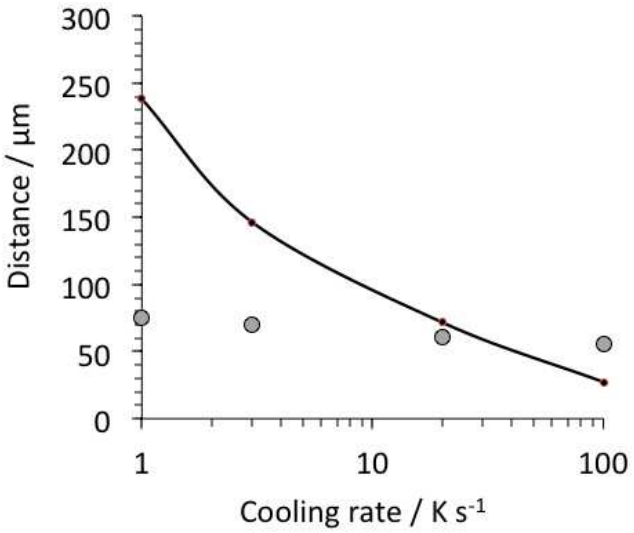

Figure 6: Comparison between average distance of interface migration (grey points) during the transformation and diffusion distance of phosphorous. The curve is calculated using grain boundary diffusivity where the flux is parallel to the boundary.

4. Conclusions

Phosphorous segregation at ferrite grain boundaries in a Fe-0.17P wt% has been investigated as a function of heat treatment. It has been demonstrated that the segregation is insensitive to the cooling rate following phase transformation from the austenitic condition. Instead, the evidence strongly suggests that the segregation occurs *during* the course of phase transformation, and there is little or no subsequent segregation as the ferrite cools to ambient temperature over the range of parameters studied. The results of a variety of heat treatments are consistent with this interpretation, and it is further demonstrated that the rate at which the ferrite forms is reasonably aligned with that at which the phosphorus may move with the transformation front.

A consequence of this study is that it will not be possible to suppress grain boundary segregation in high-phosphorus alloys using cooling rates that are practically achievable.

Acknowledgements: The authors are grateful to POSCO for support through Steel Innovation Programme.

References

[1] D. McLean: Grain Boundaries in Metals: Clarendon Press, Oxford, 1957.

[2] M. Guttmann: Surface Science 53 (1975) 213–227.

[3] E. D. Hondros, M. P. Seah: International Metals Reviews 22 (1977) 262–301.

[4] X. Tingdong, C. Buyuan: Progress in Materials Science 49 (2004) 109–208.

[5] M. Vsianska, M. Sob: Progress in Materials Science 56 (2011) 817–840.

[6] H. K. D. H. Bhadeshia: Progress in Materials Science 57 (2012) 268–435.

[7] M. J. Xu, H. Lu, C. Yu, J. J. Xu, J. M. Chen: Science and Technology of Welding and Joining 18 (2013) 184–190.

[8] C. J. McMahon Jr: Materials Science and Engineering 25 (1976) 233–239.

[9] H. Erhart, H. J. Grabke: Metal science 15 (1981) 401–408.

[10] A. K. Cianelli, H. C. Feng, A. H. Ucisik, C. J. McMahon: Metallurgical Transactions A 8 (1977) 1059–1061.

[11] G. L. Krasko, G. B. Olson: Solid State Communications 76 (1990) 247–251.

[12] A. V. Nikolaeva, Y. A. Nikolaev, Y. R. Kevorkyan: Atomic Energy 91 (2001) 534–542.

[13] S. Takayama, T. Ogura, S. C. Fu, C. J. McMahon: Metallurgical Transactions A 11 (1980) 1513–1530.

[14] R. M. Horn, R. O. Ritchie: Metallurgical Transactions A 9 (1978) 1039–1053.

[15] H. K. D. H. Bhadeshia, D. V. Edmonds: Metal Science 13 (1979) 325–334.

[16] J. A. Peters, J. V. Bee, B. Kolk, G. G. Garrett: Acta Materialia 37 (1995) 675–686.

[17] C. L. Li, D. J. Cheng, Z. H. Jin: Scripta Materialia 35 (1996) 1147–1152.

[18] J. L. Song, S. B. Lin, C. L. Yang, C. L. Fan, G. C. Ma: Science and Technology of Welding and Joining 15 (2010) 213–218.

[19] W. S. Ko, J. Y. Park, J. Y. Byun, J. K. Lee, N. J. Kim, B. J. Lee: Scripta Materialia 68 (2012) 329–332.

[20] W. S. Ko, J. B. Jeon, C. H. Lee, J. K. Lee, B. J. Lee: Modelling and Simulation in Materials Science and Engineering 21 (2013) 025012.

[21] L. Cheng, M. Enomoto, D. Hirakami, T. Tarui: ISIJ International 53 (2013) 131–138.

[22] P. Ghosh, C. Ghosh, R. K. Ray: ISIJ International 49 (2009) 1080–1086.

[23] S. Hong, S. Y. Shin, J. Lee, C. H. Lee, S. Lee: Materials Science & Engineering A A564 (2013) 461–472.

[24] S. Hong, J. Lee, K. S. Park, S. Lee: Materials Science & Engineering A http://dx.doi.org/10.1016/j.msea.2013.09.095.

[25] J. R. Cowan, H. E. Evans, R. B. Jones, P. Bowen: Acta Materialia 46 (1998) 6565–6574.

[26] R. W. Balluffi, S. M. Allen, W. C. Carter: Kinetics of Materials: John Wiley & Sons, Inc., New Jersey, 2005.

[27] B. C. D. Cooman, J. G. Speer, I. Yu Pyshmintsev, N. Yoshinaga: Materials design: the key to modern steel products: GRIPS media, Harzburg, Germany, 2007.

[28] K. Ishida: Journal of Alloys and Compounds 235 (1996) 244–249.

[29] C. Mack: Proceedings of the Cambridge Philosophical Society 52 (1956) 246–250.

[30] J. Svoboda, F. D. Fischer, E. Gamsjäger: Acta Materialia 50 (2002) 967–977.

[31] J. W. Cahn: Acta Metallurgica 10 (1962) 789–798.

[32] F. Christien, R. L. Gall: Surface Science 605 (2011) 1711–1718.

[33] C. R. Hutchinson, R. E. Hackenberg, G. J. Shiflet: Acta Materialia 52 (2004) 3565–3585.

[34] H. S. Zurob, D. Panahi, C. R. Hutchinson, Y. Brechet, G. R. Purdy: Metallurgical & Materials Transactions A 44 (2013) 3456–3471.

[35] C. W. Sinclair, C. R. Hutchinson, Y. Bréchet: Metallurgical & Materials Transactions A 38 (2007) 821–830.

[36] J. Svoboda, E. Gamsjäger, F. D. Fischer, Y. Liu, E. Kozeschnik: Acta Materialia 59 (2011) 4775–4786.

[37] J. Svoboda, J. Vala, E. Gamsjäger, F. D. Fischer: Acta Materialia 54 (2006) 3953–3960.

[38] H. N. Han, S. J. Kim, M. Kim, G. Kim, D. W. Suh, S. J. Kim: Philosophical Magazine 88 (2008) 1811–1824.

[39] M. Hillert, G. Purdy: Acta Metallurgica 26 (1978) 333–340.

[40] K. Smidoda, C. Gottschalk, H. Gleiter: Metal Science 13 (1979) 146–148.

[41] L. Chongmo, M. Hillert: Acta Metallurgica 30 (1982) 1133–1145.